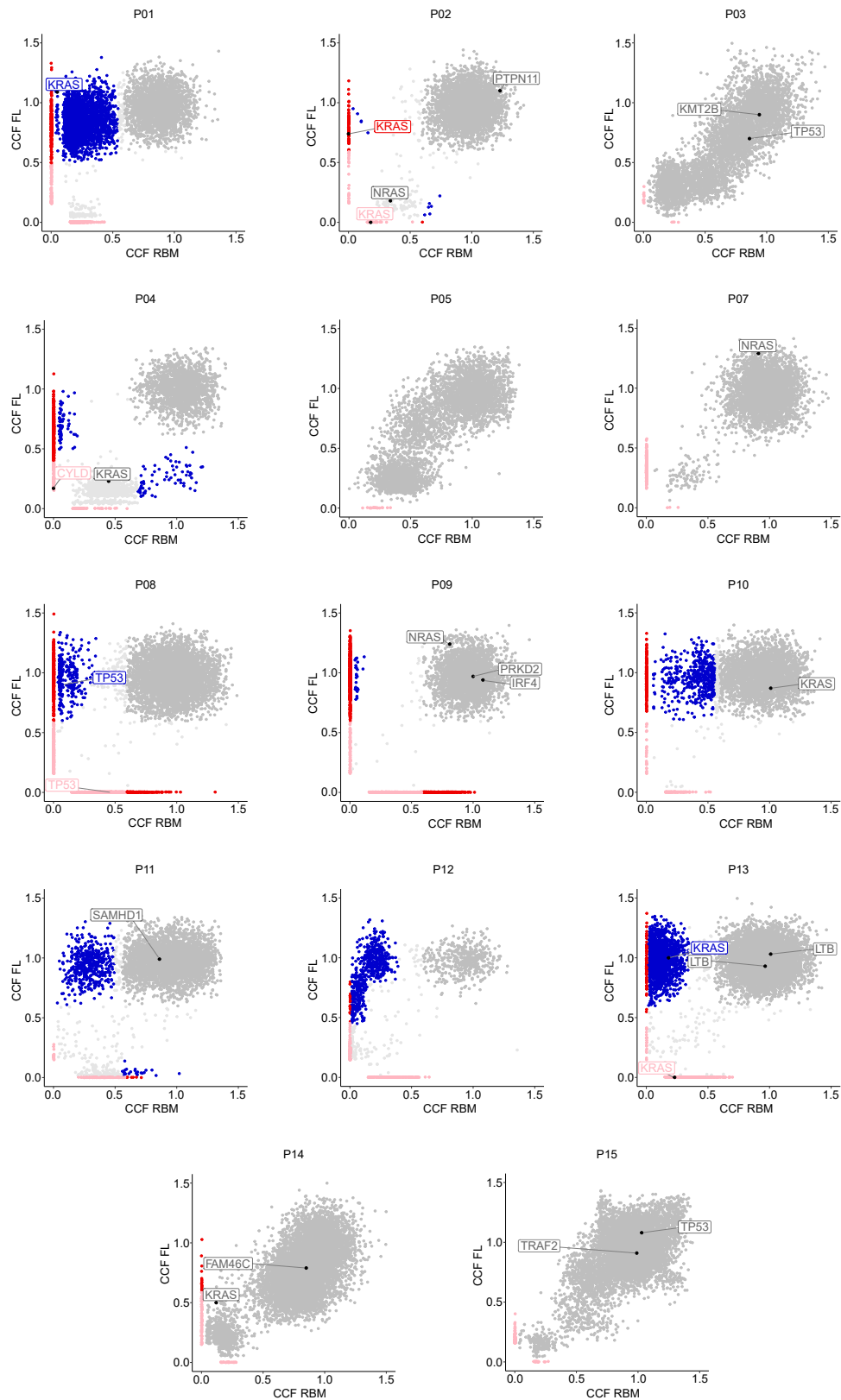


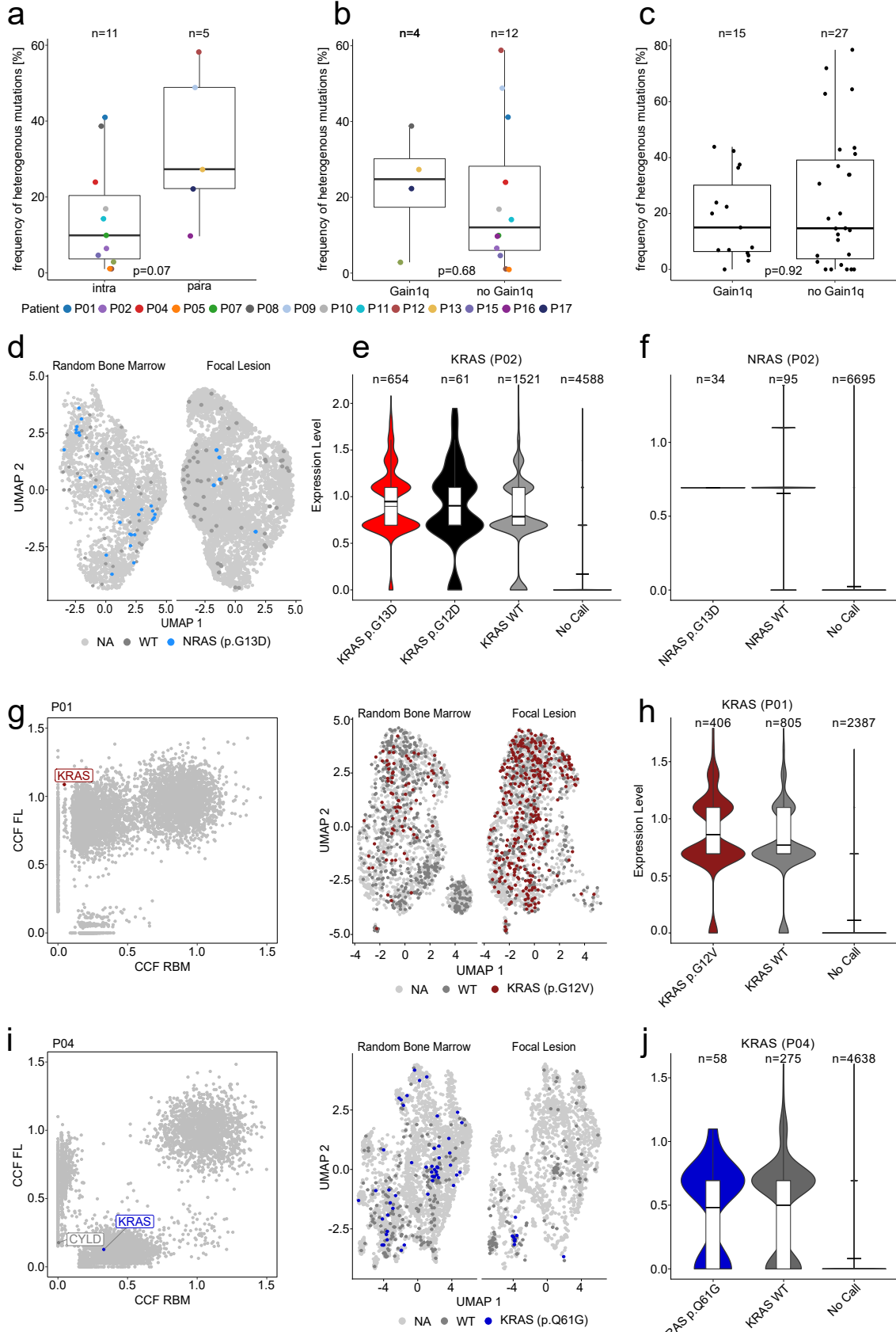
# **Resolving the Spatial Architecture of Myeloma and its Microenvironment at the Single-Cell Level**

## **Supplementary information**

### **Supplementary Figures**

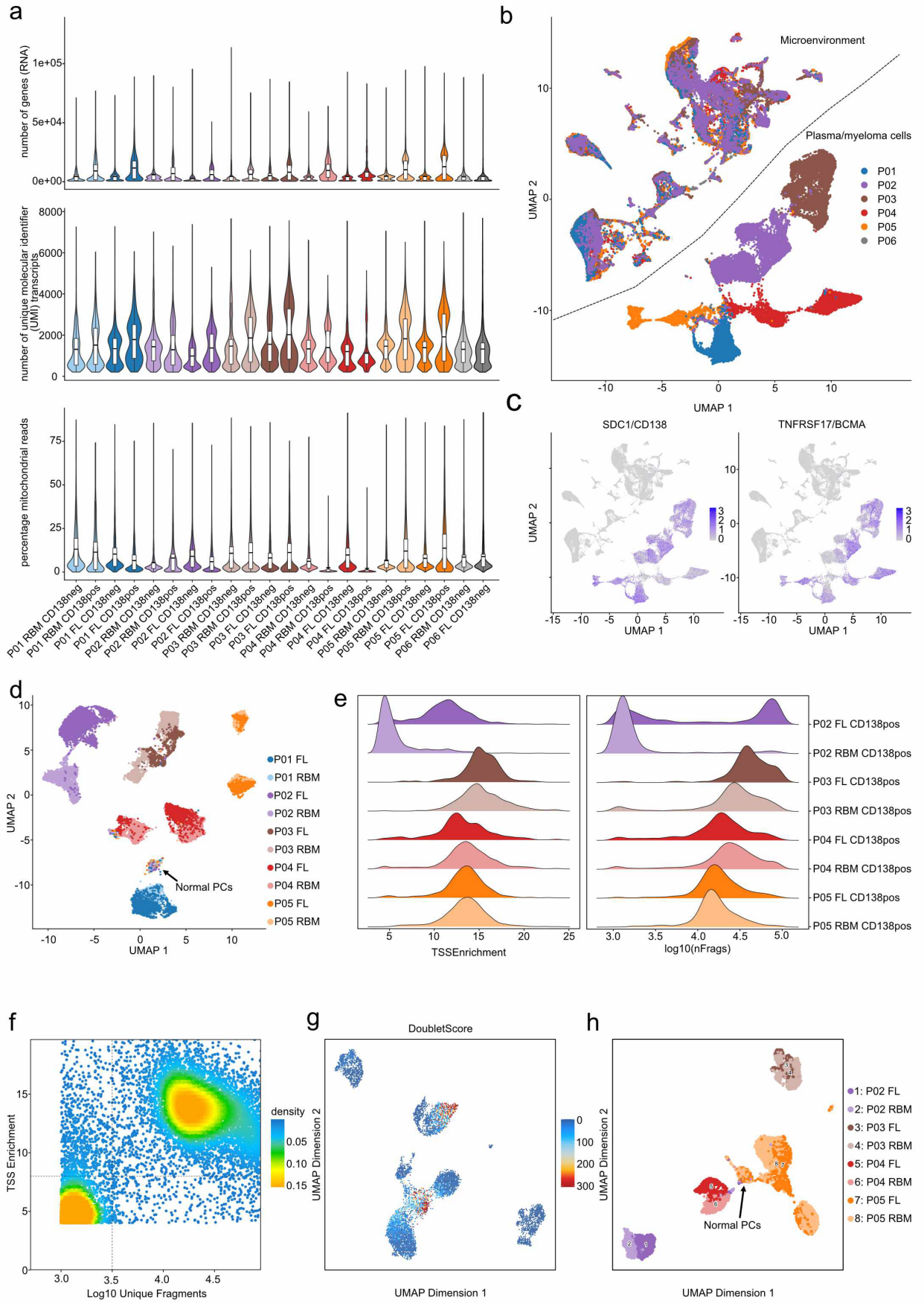


**Suppl. Fig. 1: Cancer clonal fraction (CCF) plots of paired samples.** Major and minor events between paired random bone marrow (RBM) and focal lesions (FL) were discriminated based on the 95% confidence intervals (95% CI). Mutations were classified as major (*red*), if the upper band of the 95% CI was  $\geq 1$ , and minor (*pink*) otherwise. Furthermore, major mutations with a 3-fold enrichment between the paired samples were classified as enriched (*blue*). Nonsynonymous SNVs in driver genes<sup>1</sup> are highlighted. Source data are provided as a Source Data file.



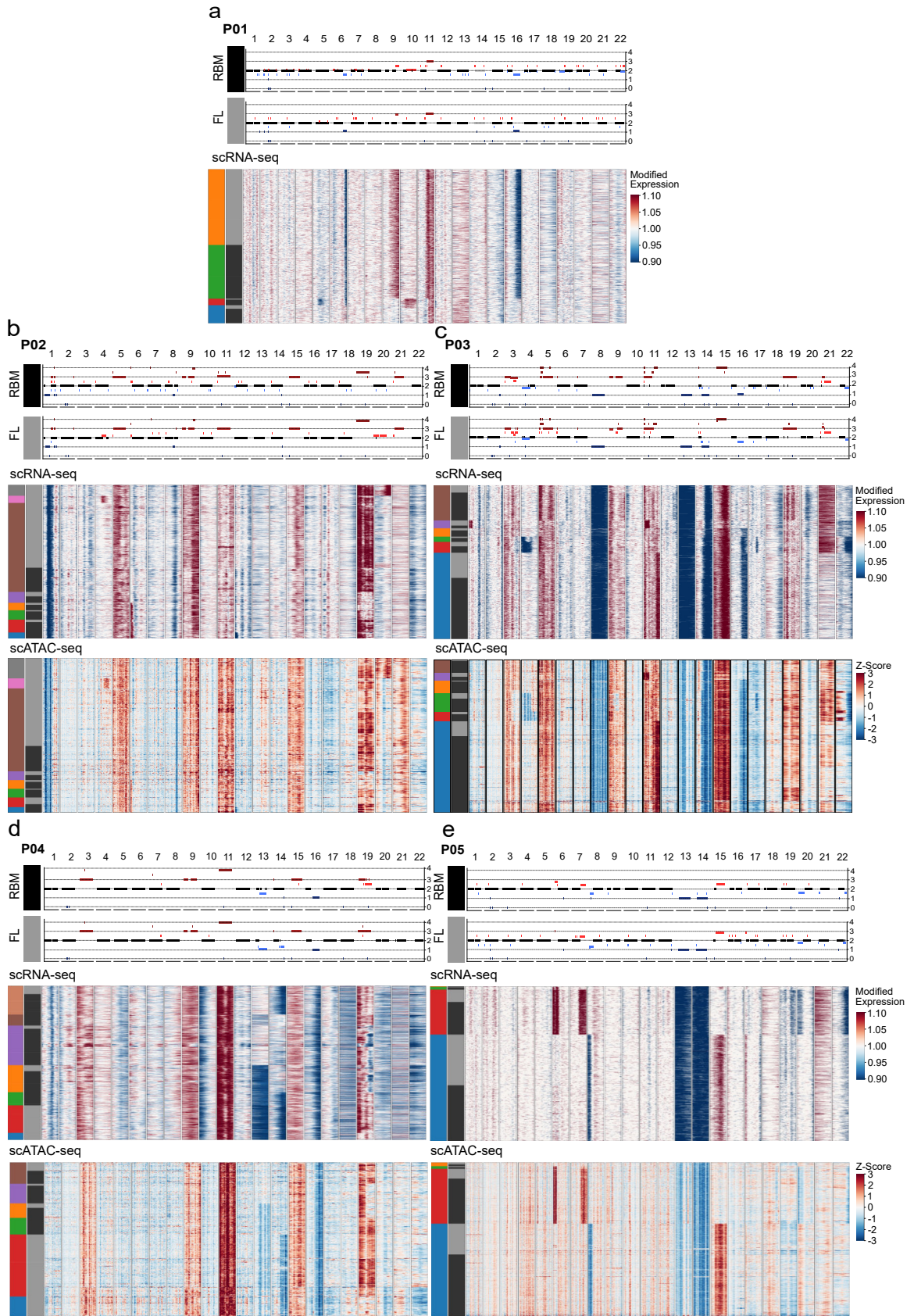
(legend on next page)

**Suppl. Fig. 2: Frequency of heterogeneous mutations in patient subgroups and *KRAS* mutation calling in whole genome and single-cell RNA-seq data.** (a) Frequency of heterogeneous mutations (unshared+enriched) in intra- vs. paramedullary samples (n=16 patients). The p-value was calculated using two-sided Wilcoxon rank sum test. (b-c) Frequency of heterogeneous mutations (unshared+enriched) in patients with gain 1q vs. patients with no gain 1q in the Heidelberg cohort (b, n=16 patients) and the UAMS patient cohort (c, n=42 patients). The p-value was calculated using two-sided Wilcoxon rank sum test. (d) Uniform Manifold Approximation and Projection (UMAP) and single-cell calls for the *NRAS* (p.G13D) mutation in patient P02. Blue dots denote cells with a *NRAS* mutation, dark gray dots denote cells with *NRAS* wild type (WT), light grey dots indicate cells with no *NRAS* call. (e-f) Violin plot of *KRAS* expression in cells with or without called *KRAS*-mutation (e) and *NRAS* expression in cells with or without *NRAS*-calls (f) in patient P02. (g) Whole genome sequencing (WGS) cancer clonal fraction (CCF) plot for single-nucleotide variants (SNVs) in paired random bone marrow (RBM) and focal lesion (FL) specimens from patient P01. The patient presented with *KRAS* (p.G12V), which was a major mutation at the FL site and a minor mutation at the RBM site. The mutation was called using scRNA-seq and positive calls are marked in the UMAP of paired RBM/FL scRNA-seq data (red, right panel). (h) Violin plot of expression of *KRAS* in cells with or without called *KRAS*-mutations in patient P01. (i) The same plots are shown for patient P04. The patient presented with a *KRAS* (p.Q61G) mutation, which was more frequent at the RBM site. Positive calls are depicted in darkblue in the scRNA-seq UMAP. (j) Violin plot of expression of *KRAS* in cells with or without called *KRAS*-mutation in patient P04. The boxplots show the median and the interquartile range, while the upper and lower whiskers show the highest and lowest value. Source data are provided as a Source Data file.



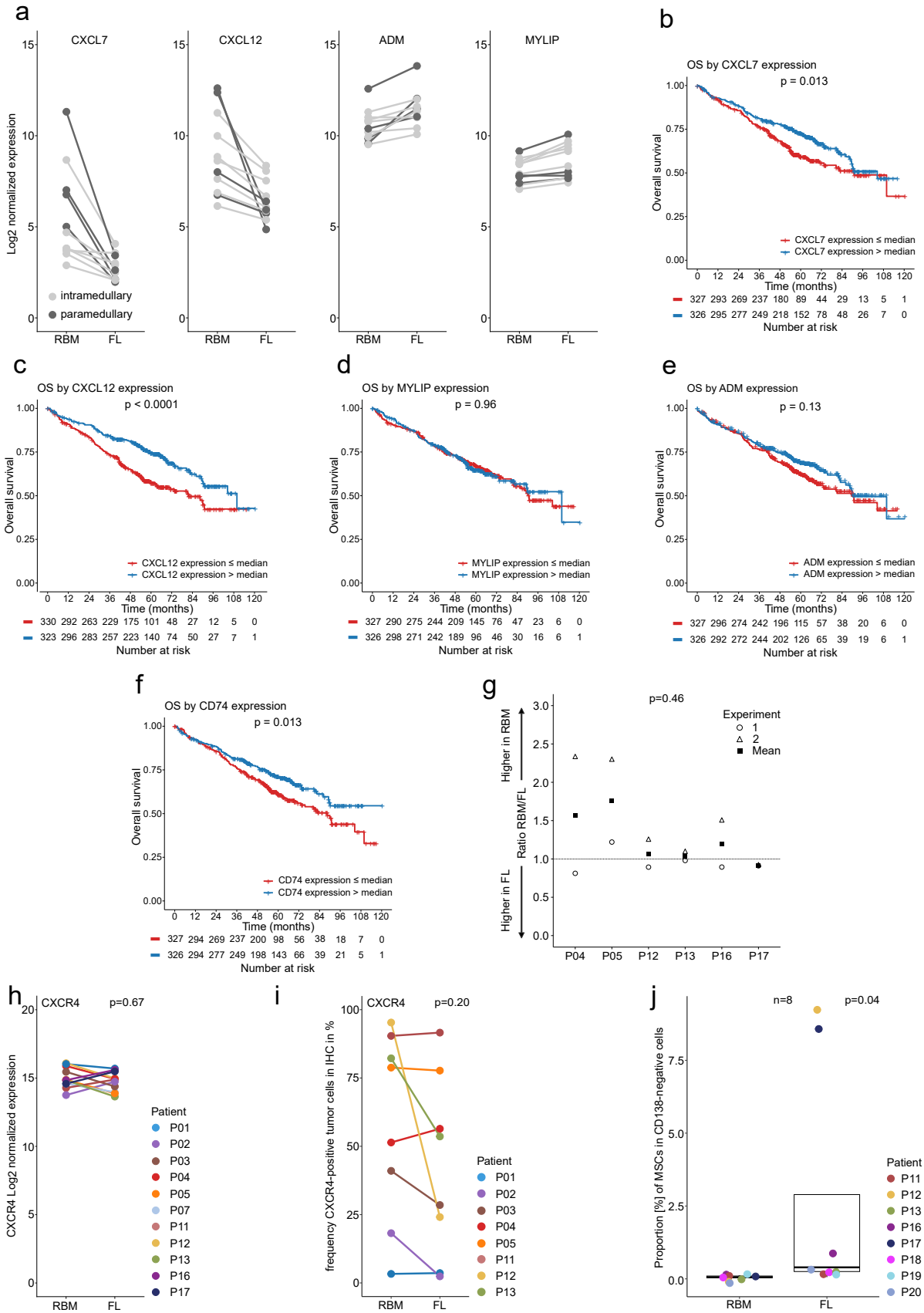
(legend on next page)

**Suppl. Fig. 3: Quality control of scRNA-seq (a-d) and scATAC-seq (e-h) data.** (a) Violin and box-whisker plot of the number of informative genes, number of unique molecular identifier (UMI) transcripts and percentage of mitochondrial reads per single cell per experimental sample to define quality control (QC) thresholds. Cells with more than 5% mitochondrial RNA, less than 200 or more than 5000 expressed genes were removed. Cell numbers before and after QC are provided in Suppl. Table 7. The boxplots show the median and the interquartile range, while the upper and lower whiskers show the highest and lowest value. (b) UMAP of all 74,631 cells after QC coloured by patients. (c) Feature plot of the expression of the two plasma cell marker genes CD138 (SDC1) and BCMA (TNFRSF17) to split the dataset into plasma cells (CD138-positive) and cells from the tumor microenvironment (TME, CD138-negative). (d) UMAP of CD138-positive myeloma/plasma cells from paired random bone marrow (light colors) and focal lesion (dark colors) specimens from 5 newly diagnosed patients. The multicolored cluster (arrow) corresponds to normal plasma cells which were used as a reference for CNA-calling. (e) Distribution of transcription start site (TSS) enrichment scores and number of unique nuclear fragments for each single cell before filtering (scATAC-seq). (f) scATAC-seq QC filtering plot for all RBM and FL patient samples showing the TSS enrichment score vs unique nuclear fragments per cell. Dot colour represents the density in arbitrary units of points in the plot. Dashed lines represent the filters for high-quality scATAC-seq data (3,000 unique nuclear fragments and TSS score greater than or equal to 8). (g) UMAPs of scATAC-seq data coloured by the per-cell doublet score to define filtering thresholds. (h) UMAPs of the filtered scATAC-seq data coloured by patient and sample. The arrow marks the cluster of normal plasma cells used as reference for CNA-calling.



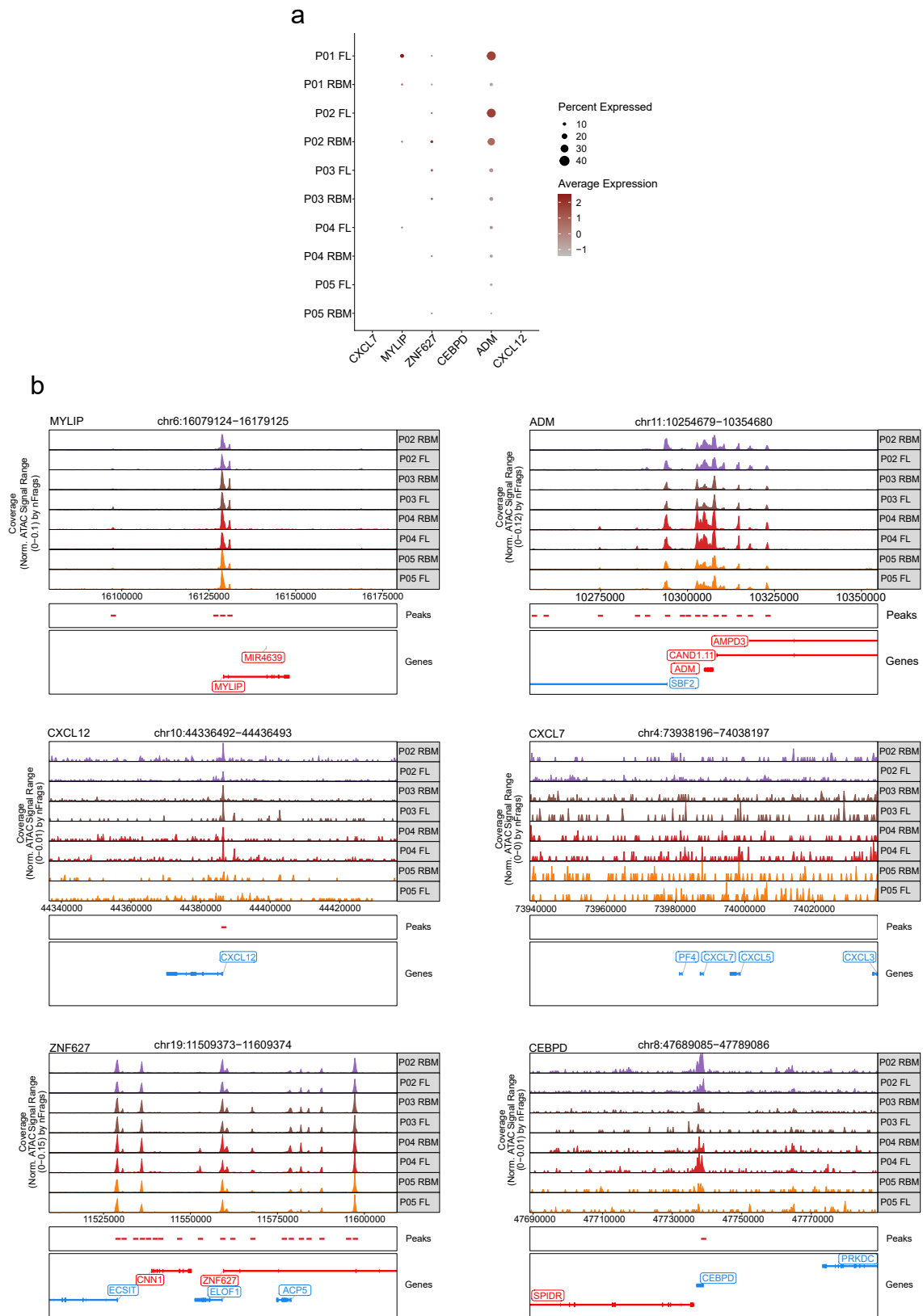
(legend on next page)

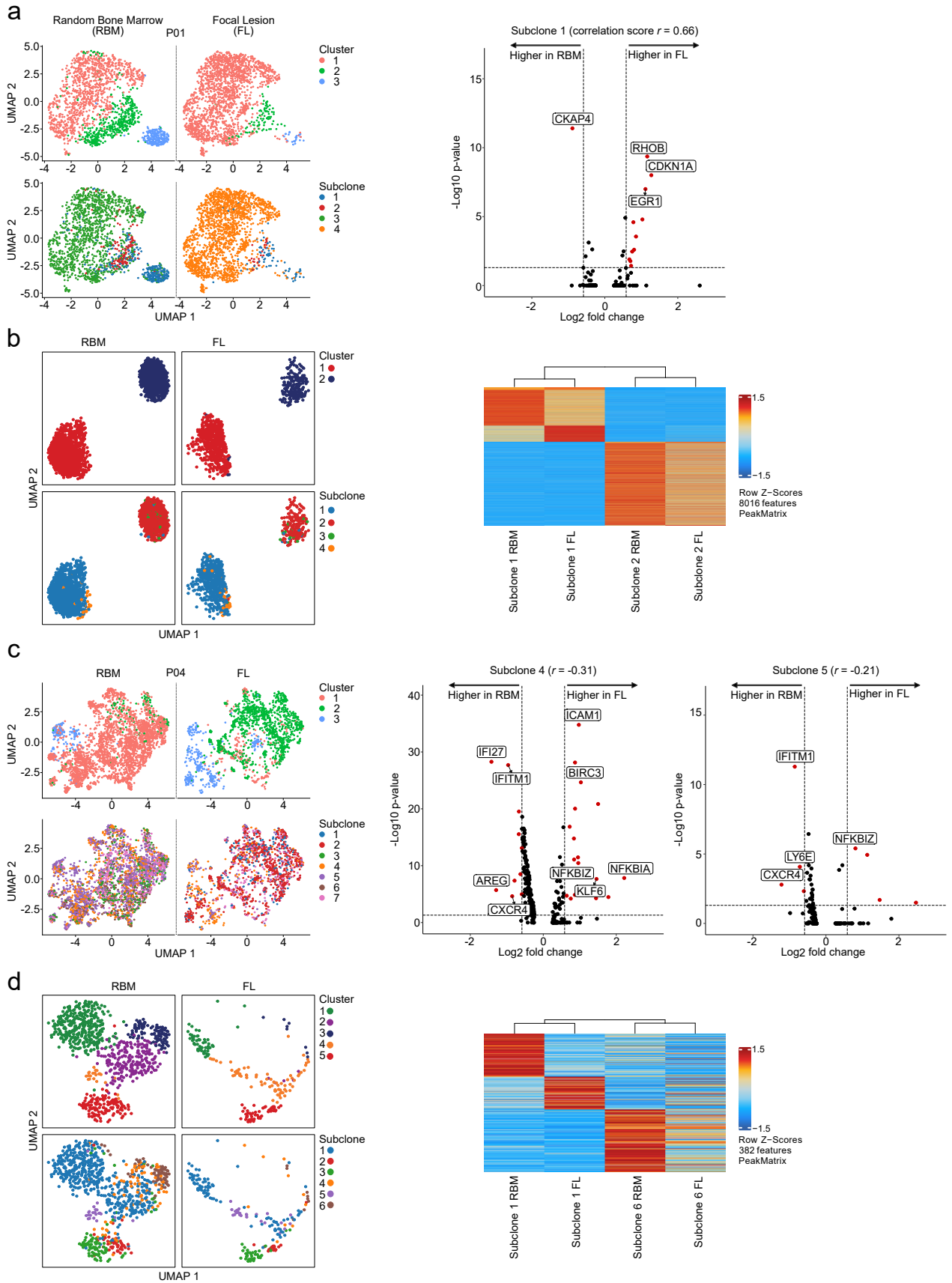
**Suppl. Fig. 4: Copy number aberration defined subclones in single-cell data.** (a)-(e) In the upper panel of each plot the whole genome sequencing chromosomal profiles for each autosomal chromosome in paired RBM (*black* bar) and focal lesion (FL) (*gray* bar) specimens are depicted. *Light red* and *light blue* denote subclonal chromosomal gains and losses, respectively. Clonal events are marked with *dark red* and *dark blue*. To identify subclones, the average relative gene expression/accessibility in regions impacted by subclonal events was used for supervised clustering of scRNA-seq (middle panel) and scATAC-seq (lower panel) data of paired RBM (*black* bar) and FL (*gray* bar) samples. In the heatmaps *red* and *blue* signals correspond to higher and lower gene expression/accessibility, respectively. The detected subclones are depicted on the left side of the two heatmaps in different colors. For P01 no scATAC-seq data was available.



(legend on next page)

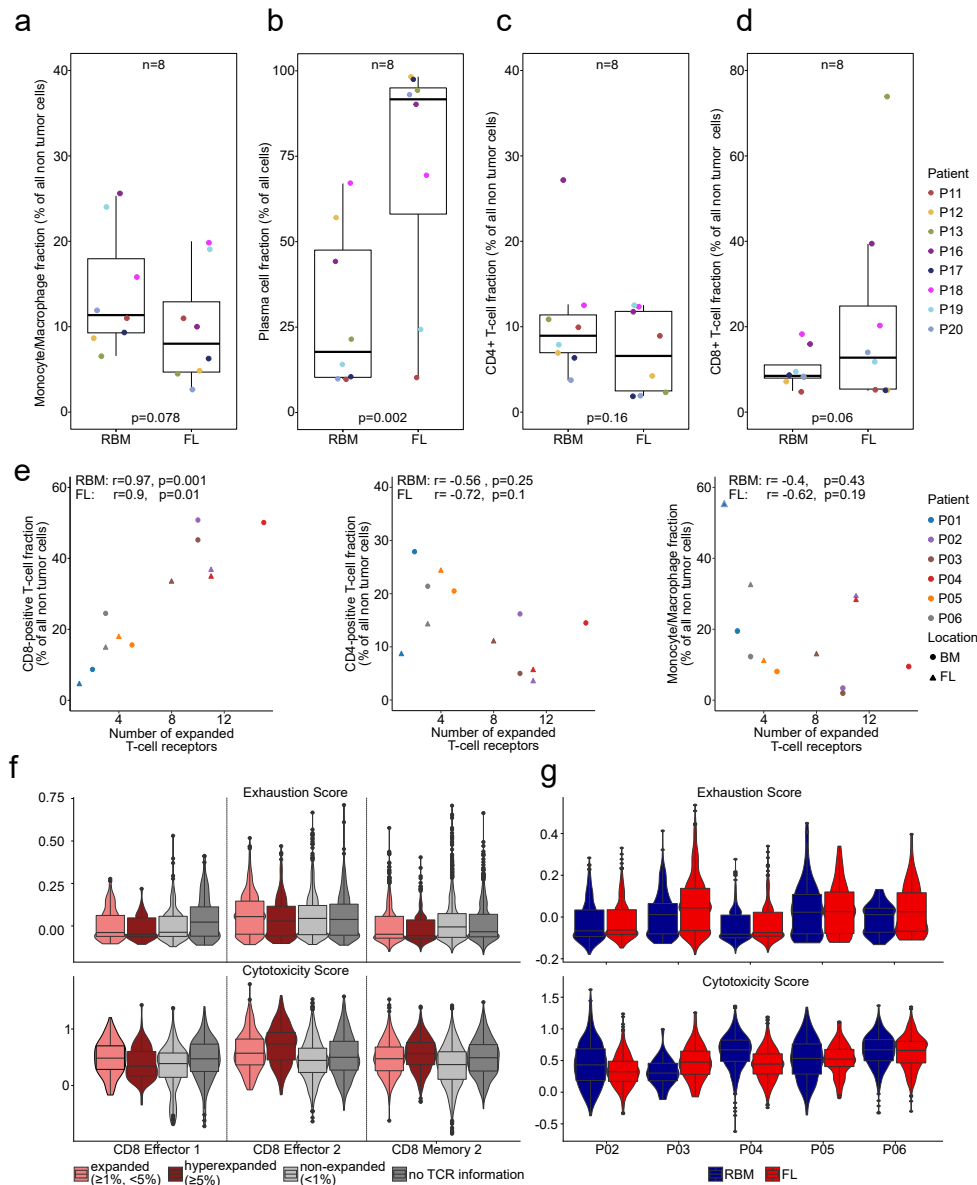
**Suppl. Fig. 5: Comparison of chemokine expression in different subgroups and expression differences in RNA-seq, ELISA and immunohistochemistry** (a) Comparison of gene expression between intra- (light grey) and paramedullary (dark grey) samples for CXCL7 (PPBP), CXCL12, ADM and MYLIP. (b-f) Overall survival (OS) of 653 newly diagnosed multiple myeloma patients<sup>2</sup> stratified by the median expression of (b) CXCL7 (PPBP), (c) CXCL12, (d) MYLIP, (e) ADM or (f) CD74. P-values were calculated based on log-rank test. (g) Protein expression of CXCL12 based on ELISA. Ratios between random samples and focal lesions are plotted for 6 patients (n=2 replicates, the p-value was calculated with a linear mixed-effects model). (h) Line plot for the log<sub>2</sub>-normalized bulk RNA-seq expression values of CXCR4 are shown. The p-value was calculated with the two-sided Wald-test in DESeq2 and corrected for multiple testing using Benjamini-Hochberg method. (i) Line plot showing the proportion of CXCR4-positive plasma cells in the focal lesion compared to the random sample per patient (n=8 patients with bulk RNA-seq data) based on immunohistochemistry staining. The p-value was calculated with two-sided Wilcoxon signed rank test. (j) Boxplot for the proportion of mesenchymal stroma cells (MSCs) according to flow cytometry for 8 patients with paired RBM/FL. Proportions were calculated based on the CD138-depleted fractions. The p-value was calculated with two-sided Wilcoxon signed rank test. The boxplots show the median and the interquartile range, while the upper and lower whiskers show the highest and lowest value. Source data are provided as a Source Data file.



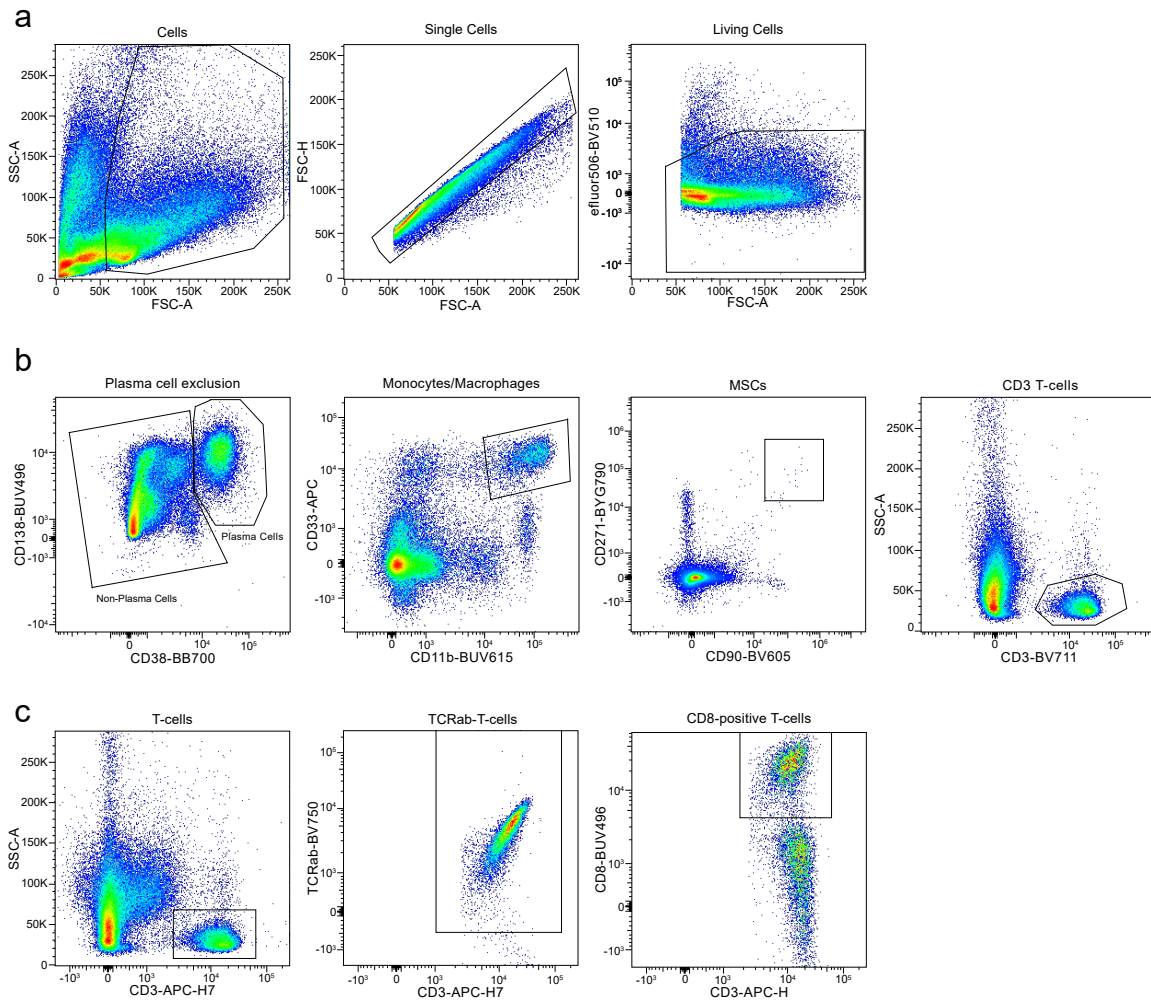


(legend on next page)

**Suppl. Fig. 7: Spatial transcriptional and epigenetic plasticity in tumor subclones.** (a) *Left panel:* Uniform Manifold Approximation and Projection (UMAP) of transcriptional clusters and CNA-subclones in patient P01 split by BM-site (random bone marrow (RBM) and focal lesion (FL)). *Right panel:* Volcano Plots of the differentially expressed genes between FL and RBM of subclones with >50 cells at both BM-sites. Red points indicate genes with an adjusted p-value<0.05 and 1.5-fold expression difference between both sites. (b) Single-cell ATAC-seq data for patient P05 as an example for very similar chromatin accessibility profiles of genetically identical subclones in paired samples. *Left panel:* chromatin accessibility clusters and copy number aberration (CNA)-defined subclones *Right panel:* scATAC-seq heatmap of differential accessibility peaks across subclones. Color indicates the column Z-score of normalized peak accessibility. (c) *Left panel:* Uniform Manifold Approximation and Projection (UMAP) of transcriptional clusters and CNA-subclones in patient P04 split by BM-site (random bone marrow (RBM) and focal lesion (FL)). *Right panel:* Volcano Plots of the differentially expressed genes between FL and RBM of subclones with >50 cells at both BM-sites. Red points indicate genes with an adjusted p-value of <0.05 and 1.5-fold expression difference between both sites. (d) In (d) the same plots as in (b) are shown for patient P03 as an example for pronounced differences between genetically identical subclones at different bone marrow sites. The two subclones 1 and 6 were assigned to different chromatin accessibility clusters at the FL and the RBM, suggesting differential chromatin accessibility profiles of the same subclone at different bone marrow sites. Of note, the cell number of subclone 6 in the FL was <50 cells. P-values were calculated based on two-sided Wilcoxon rank sum test and Benjamini-Hochberg adjustment.



**Suppl. Fig. 8: Spatial heterogeneity in the microenvironment and T-cell receptor repertoire.** (a) Boxplot for the proportion of macrophages according to flow cytometry for 8 patients with paired RBM/FL samples. Proportions were calculated based on the CD138-depleted fractions. (b) Boxplot of the plasma cell infiltration of 8 patients with paired RBM/FL samples according to flow cytometry. (c,d) Boxplots for the proportion of CD4- (c) and CD8-positive (d) T-cells according to flow cytometry for 8 patients with paired RBM/FL samples. Proportions were calculated based on the CD138-depleted fractions. All p-values were calculated with two-sided Wilcoxon signed rank test. (e) Association between the number of expanded T-cell clones (x-axis) and the proportion of CD8- (left), CD4-positive T-cells (middle) and macrophages (right) (y-axis) for all 6 patients with scRNA-seq data. Each sample was plotted separately and colored by patient and location. The correlation was separately tested for focal lesion and random bone marrow samples using Pearson correlation. (f) Recently published T-cell exhaustion and cytotoxicity scores<sup>2</sup> were calculated for CD8 effector 1 and 2 as well as CD8 memory 2 T-cells for all patients with TME scRNA-seq data combined. No significant difference could be observed between (hyper-)expanded and non-expanded T-cells. (NA: no T-cell receptor information available). (g) T-cell exhaustion and cytotoxicity scores for expanded T-cells (≥1%) splitted by sample origin for all patients with TME scRNA-seq data combined. Cell numbers are provided in the Source Data (f-g). The boxplots show the median and the interquartile range, while the upper and lower whiskers show the highest and lowest value. Source data are provided as a Source Data file.



**Suppl. Fig. 9: Gating strategy flow cytometry analysis.** (a) Gating strategy to identify living cells for downstream analysis. (b) Plasma cells were identified as CD38<sup>+</sup> CD138<sup>+</sup> (see Suppl. Fig. 8b) and were excluded from further gating. Monocytes/macrophages were defined as CD11b<sup>+</sup> CD33<sup>+</sup> (see Suppl. Fig. 8a), mesenchymal stromal cells as CD90<sup>+</sup> CD271<sup>+</sup> (see Suppl. Fig. 5j) and T-cells as CD3<sup>+</sup>. (c) T-cell focus. CD8<sup>+</sup> T-cells were defined as CD3<sup>+</sup>, TCRab<sup>+</sup> and CD8<sup>+</sup> (see Suppl. Fig. 8c+d). For the analysis of (b) and (c) the sample was analyzed in two tubes: one tube for a general cell type annotation and the second one to define subsets of T-cells.

## Supplementary Tables

**Suppl. Table 1:** Driver mutations of all samples included in this study.

| PID | Group        | Driver mutations*  |
|-----|--------------|--|
| P01 | Shared       | -  |
| P01 | Enriched RBM | -  |
| P01 | Enriched FL  | <i>KRAS</i> <sup>G35T</sup>  |
| P02 | Shared       | <i>PTPN11</i> <sup>C1520A</sup>  |
| P02 | Enriched RBM | <i>KRAS</i> <sup>G35A</sup> , <i>NRAS</i> <sup>G38A</sup>  |
| P02 | Enriched FL  | <i>KRAS</i> <sup>G38A</sup> , <i>CDKN2C</i> <sup>T365C/del</sup>   |
| P03 | Shared       | <i>KMT2B</i> <sup>G413A</sup> , <i>TP53</i> <sup>T425A</sup> , <i>RB1</i> <sup>del/del</sup> , <i>RASA2</i> <sup>del/del</sup> |
| P03 | Enriched RBM | -  |
| P03 | Enriched FL  | -  |
| P04 | Shared       | -  |
| P04 | Enriched RBM | <i>KRAS</i> <sup>A183C</sup>   |
| P04 | Enriched FL  | <i>CYLD</i> <sup>G1466T/del</sup>  |
| P05 | Shared       | -  |
| P05 | Enriched RBM | -  |
| P05 | Enriched FL  | -  |
| P07 | Shared       | <i>NRAS</i> <sup>G35A</sup>  |
| P07 | Enriched RBM | -  |
| P07 | Enriched FL  | -  |
| P08 | Shared       | -  |
| P08 | Enriched RBM | <i>TP53</i> <sup>C817T/del</sup>   |
| P08 | Enriched FL  | <i>TP53</i> <sup>G538A/del</sup> , <i>RB1</i> <sup>del/del</sup> , <i>CYLD</i> <sup>del/del</sup>                              |
| P09 | Shared       | <i>NRAS</i> <sup>C181A</sup> , <i>PRKD2</i> <sup>C1676T</sup> , <i>IRF4</i> <sup>A368G</sup>                                   |
| P09 | Enriched RBM | -  |
| P09 | Enriched FL  | -  |
| P10 | Shared       | <i>KRAS</i> <sup>A183C</sup>   |
| P10 | Enriched RBM | -  |
| P10 | Enriched FL  | -  |
| P11 | Shared       | <i>SAMHD1</i> <sup>G371A</sup>   |
| P11 | Enriched RBM | -  |
| P11 | Enriched FL  | -  |
| P12 | Shared       | -  |
| P12 | Enriched RBM | -  |
| P12 | Enriched FL  | -  |
| P13 | Shared       | <i>LTB</i> <sup>G157A</sup>  |
| P13 | Enriched RBM | <i>KRAS</i> <sup>G436A</sup>   |
| P13 | Enriched FL  | <i>KRAS</i> <sup>G35C</sup>  |
| P14 | Shared       | <i>FAM46C</i> <sup>C1015T</sup>  |
| P14 | Enriched RBM | -  |
| P14 | Enriched FL  | <i>KRAS</i> <sup>A183C</sup>   |
| P15 | Shared       | <i>TRAF2</i> <sup>G1366T</sup> , <i>TP53</i> <sup>G839A</sup>  |
| P15 | Enriched RBM | -  |
| P15 | Enriched FL  | -  |
| P16 | Shared       | <i>NRAS</i> <sup>A182G</sup>   |
| P16 | Enriched RBM | -  |
| P16 | Enriched FL  | -  |
| P17 | Shared       | -  |
| P17 | Enriched RBM | -  |
| P17 | Enriched FL  | -  |

RBM: random bone marrow; FL: focal lesion;

\*Driver mutations according to Walker et al.<sup>1</sup>

Enriched means unshared or threefold difference in the cancer clonal fractions between paired samples.

**Suppl. Table 2:** Details of the linear mixed-effects model used for immunohistochemistry data.

| <b>Coefficients for CD68</b>              | <b>Estimate</b> | <b>Standard Error</b> | <b>t-value</b> | <b>p-value</b> |
|---|-----------------|-----------------------|----------------|----------------|
| (Intercept)                               | 41.04           | 2.25                  | 18.22          | <0.0001        |
| Inf2                                      | -16.30          | 2.46                  | -6.62          | <0.0001        |
| Inf3                                      | -29.06          | 2.24                  | -12.95         | <0.0001        |
| Inf4                                      | -40.25          | 1.93                  | -20.87         | <0.0001        |
| Sample RBM                                | 8.23            | 1.20                  | 6.85           | <0.0001        |
| Correlation between predictors*: $r=0.29$ |                 |                       |                |                |
| <b>Coefficients for CD4</b>               | <b>Estimate</b> | <b>Standard Error</b> | <b>t-value</b> | <b>p-value</b> |
| (Intercept)                               | 22.99           | 2.02                  | 11.39          | <0.0001        |
| Inf2                                      | -8.70           | 2.38                  | -3.65          | 0.0003         |
| Inf3                                      | -16.99          | 2.16                  | -7.86          | <0.0001        |
| Inf4                                      | -21.49          | 1.95                  | -11.03         | <0.0001        |
| Sample RBM                                | -0.94           | 1.05                  | -0.90          | 3.68 E-01      |
| Correlation between predictors*: $r=0.21$ |                 |                       |                |                |
| <b>Coefficients for CD8</b>               | <b>Estimate</b> | <b>Standard Error</b> | <b>t-value</b> | <b>p-value</b> |
| (Intercept)                               | 17.88           | 2.23                  | 8.00           | <0.0001        |
| Inf2                                      | 0.31            | 2.57                  | 0.12           | 0.91           |
| Inf3                                      | -4.92           | 2.23                  | -2.21          | 0.027          |
| Inf4                                      | -14.99          | 2.02                  | -7.41          | <0.0001        |
| Sample RBM                                | 3.86            | 1.138                 | 3.39           | 0.0006         |
| Correlation between predictors*: $r=0.19$ |                 |                       |                |                |

Inf2: 26-50% Plasma cell infiltration, Inf3:51-75% plasma cell infiltration, Inf4: 76-100% Plasma-cell infiltration.  
RBM: random bone marrow, VIF<1.1; \*for the correlation analysis numerical values for predictors were used.

**Suppl. Table 3:** Overview of samples and performed analyses per patient.

| PID | WGS | RNA bulk | scRNA tumor | scRNA TME | scATAC tumor | FACS | ELISA CXCL12 | IHC Ki67/CXCL12/ CXCR4 | IHC Monocytes/ T-cells |
|-----|-----|----------|-------------|-----------|--------------|------|--------------|------------------------|------------------------|
| P01 |     |          |             |           |              |      |              |                        |                        |
| P02 |     |          |             |           |              |      |              |                        |                        |
| P03 |     |          |             |           |              |      |              |                        |                        |
| P04 |     |          |             |           |              |      |              |                        |                        |
| P05 |     |          |             |           |              |      |              |                        |                        |
| P06 |     |          |             |           |              |      |              |                        |                        |
| P07 |     |          |             |           |              |      |              |                        |                        |
| P08 |     |          |             |           |              |      |              |                        |                        |
| P09 |     |          |             |           |              |      |              |                        |                        |
| P10 |     |          |             |           |              |      |              |                        |                        |
| P11 |     |          |             |           |              |      |              |                        |                        |
| P12 |     |          |             |           |              |      |              |                        |                        |
| P13 |     |          |             |           |              |      |              |                        |                        |
| P14 |     |          |             |           |              |      |              |                        |                        |
| P15 |     |          |             |           |              |      |              |                        |                        |
| P16 |     |          |             |           |              |      |              |                        |                        |
| P17 |     |          |             |           |              |      |              |                        |                        |
| P18 |     |          |             |           |              |      |              |                        |                        |
| P19 |     |          |             |           |              |      |              |                        |                        |
| P20 |     |          |             |           |              |      |              |                        |                        |
| P21 |     |          |             |           |              |      |              |                        |                        |
| P22 |     |          |             |           |              |      |              |                        |                        |
| P23 |     |          |             |           |              |      |              |                        |                        |
| P24 |     |          |             |           |              |      |              |                        |                        |
| P25 |     |          |             |           |              |      |              |                        |                        |
| P26 |     |          |             |           |              |      |              |                        |                        |
| P27 |     |          |             |           |              |      |              |                        |                        |
| P28 |     |          |             |           |              |      |              |                        |                        |
| P29 |     |          |             |           |              |      |              |                        |                        |
| P30 |     |          |             |           |              |      |              |                        |                        |
| P31 |     |          |             |           |              |      |              |                        |                        |

green: analysis performed with the paired random and focal lesion sample, grey: no paired samples available

**Suppl. Table 4: Patient characteristics**

| PID | Age at Diagnosis | R-ISS   | FISH-Risk              | IG Type            | Origin of focal lesion sample                | Type of investigated lesion |
|-----|------------------|---------|------------------------|--------------------|--|-----------------------------|
| P01 | <65              | I       | standard               | BJ kappa           | left iliac crest                             | intramedullary              |
| P02 | <65              | III     | standard               | IgG kappa          | right iliac crest                            | intramedullary              |
| P03 | <65              | II      | standard               | IgG kappa          | right iliac crest                            | intramedullary              |
| P04 | <65              | II      | standard               | IgG kappa          | left iliac crest                             | intramedullary              |
| P05 | <65              | I       | standard               | Light chain lambda | right iliac crest                            | intramedullary              |
| P06 | <65              | I       | standard               | IgA kappa          | left iliac crest                             | intramedullary              |
| P07 | <65              | I       | standard               | IgA kappa          | right iliac crest                            | intramedullary              |
| P08 | <65              | II      | amp(1q21)<br>del(17p)  | IgA kappa          | left iliac crest                             | intramedullary              |
| P09 | >65              | II      | standard               | IgA lambda         | right humerus (surgical resection)           | paramedullary               |
| P10 | >65              | I       | standard               | BJ lambda          | right iliac crest                            | intramedullary              |
| P11 | <65              | I       | standard               | IgG kappa          | left iliac crest                             | intramedullary              |
| P12 | <65              | I       | standard               | BJ lambda          | 3rd cervical vertebra (surgical resection)   | paramedullary               |
| P13 | >65              | NA      | gain(1q21)             | IgA kappa          | 2nd lumbal vertebra (surgical resection)     | paramedullary               |
| P14 | <65              | I       | gain(1q21)             | IgG kappa          | left iliac crest                             | intramedullary              |
| P15 | >65              | III     | standard               | IgG kappa          | left iliac crest                             | intramedullary              |
| P16 | <65              | I       | standard               | IgG kappa          | 1st lumbal vertebra (surgical resection)     | paramedullary               |
| P17 | >65              | I       | gain(1q21)             | BJ kappa           | 6/7th cervical vertebra (surgical resection) | paramedullary               |
| P18 | <65              | II      | standard               | IgG kappa          | left iliac crest                             | intramedullary              |
| P19 | <65              | I       | gain(1q21)             | IgG kappa          | left iliac crest                             | intramedullary              |
| P20 | >65              | II      | standard               | IgG kappa          | 2nd lumbal vertebra (surgical resection)     | paramedullary               |
| P21 | <65              | III     | t(4;14)+<br>gain(1q21) | IgA kappa          | 5. thoracic vertebra                         | paramedullary               |
| P22 | >65              | ISS III | unknown                | IgG kappa          | Left proximal femur (surgical resection)     | intramedullary              |
| P23 | <65              | I       | standard               | IgG kappa          | right sacrum                                 | intramedullary              |
| P24 | >65              | I       | standard               | BJ lambda          | right pubis                                  | intramedullary              |
| P25 | <65              | III     | gain(1q21)             | IgG lambda         | left iliac crest                             | paramedullary               |
| P26 | >65              | ISS I   | unknown                | Light chain lambda | left ulna                                    | intramedullary              |
| P27 | <65              | II      | t(4;14)+<br>gain(1q21) | IgG lambda         | left ilium                                   | intramedullary              |
| P28 | <65              | I       | standard               | IgG kappa          | right femur neck (surgical resection)        | intramedullary              |
| P29 | <65              | ISS II  | unknown                | IgG lambda         | right ilium                                  | intramedullary              |
| P30 | >65              | II      | standard               | IgG kappa          | left ilium                                   | intramedullary              |
| P31 | <65              | II      | standard               | BJ lambda          | left humerus                                 | intramedullary              |

PID: patient identifier; R-ISS: revised international staging system; FISH-Risk (random iliac crest sample): gain(1q), del(17p), t(4;14) and t(14;16) were considered as high-risk markers; IG: Immunoglobulin; BJ: Bence Jones

**Suppl. Table 5:** Sample processing and purity.

| PID | Random sample |                |               | Focal Lesion       |                              |               |
|-----|---------------|----------------|---------------|--------------------|------------------------------|---------------|
|     | Sample type   | Sorting Method | Purity (WGS)* | Sample type        | Sorting method               | Purity (WGS)* |
| P01 | Aspirate      | Robosep        | 0.9           | Aspirate           | Robosep                      | 0.8           |
| P02 | Aspirate      | Robosep        | 0.96          | Aspirate           | Robosep                      | 0.92          |
| P03 | Aspirate      | Robosep        | 1             | Aspirate           | Robosep                      | 1             |
| P04 | Aspirate      | Robosep        | 0.92          | Aspirate           | Robosep                      | 0.98          |
| P05 | Aspirate      | Robosep        | 0.78          | Aspirate           | Robosep                      | 0.8           |
| P06 | Aspirate      | Robosep        | NA            | Aspirate           | Robosep                      | NA            |
| P07 | Aspirate      | Robosep        | 0.98          | Aspirate           | Robosep                      | 0.86          |
| P08 | Aspirate      | Robosep        | 0.9           | Aspirate           | Robosep                      | 0.84          |
| P09 | Aspirate      | Robosep        | 0.96          | Surgical resection | fresh-frozen tissue, no sort | 0.84          |
| P10 | Aspirate      | Robosep        | 0.82          | Aspirate           | Robosep                      | 0.92          |
| P11 | Aspirate      | Robosep        | 0.52          | Aspirate           | Robosep                      | 0.9           |
| P12 | Aspirate      | Robosep        | 0.98          | Surgical resection | FACSAria                     | 0.98          |
| P13 | Aspirate      | Robosep        | 0.88          | Surgical resection | FACSAria                     | 0.98          |
| P14 | Aspirate      | Robosep        | 0.98          | Aspirate           | Robosep                      | 0.91          |
| P15 | Aspirate      | Robosep        | 1             | Aspirate           | Robosep                      | 1             |
| P16 | Aspirate      | Robosep        | 0.86          | Surgical resection | FACSAria                     | 0.98          |
| P17 | Aspirate      | Robosep        | 0.7           | Surgical resection | FACSAria                     | 0.98          |

WGS: whole genome sequencing

\* The tumor purity was estimated based on histograms for the variant allele frequency (VAF) of mutations according to whole genome sequencing

**Suppl. Table 6: Antibodies used for flow cytometry or immunohistochemistry stainings**

| Antibody                           | Tube | Method         | Conjugate  | Clone       | Dilution     | Source          | Cat#     | Validated* |
|------------------------------------|------|----------------|------------|-------------|--------------|-----------------|----------|------------|
| Mouse anti-human CD3               | 1    | Flow cytometry | BV711      | SK7         | 1:100        | BD Biosciences  | 740832   | yes        |
| Rat anti-human CD11b               | 1    | Flow cytometry | BUV615     | M1/70       | 1:50         | BD Biosciences  | 751140   | yes        |
| Mouse anti-human CD33              | 1    | Flow cytometry | APC        | WM53        | 1:20         | BD Biosciences  | 551378   | yes        |
| Mouse anti-human CD34              | 1    | Flow cytometry | PE         | 581         | 1:5          | BD Biosciences  | 555822   | yes        |
| Mouse anti-human CD38              | 1    | Flow cytometry | PerCPCy5.5 | HIT2        | 1:100        | BD Biosciences  | 551400   | yes        |
| Mouse anti-human CD45RA            | 1    | Flow cytometry | BB515      | HI100       | 1:100        | BD Biosciences  | 564552   | yes        |
| Mouse anti-human CD90              | 1    | Flow cytometry | BV605      | 5E10        | 1:50         | BD Biosciences  | 747750   | yes        |
| Mouse anti-human CD138             | 1    | Flow cytometry | BUV496     | MI15        | 1:50         | BD Biosciences  | 749874   | yes        |
| Mouse anti-human CD271             | 1    | Flow cytometry | PE-Cy7     | ME20.4-1.H4 | 1:50         | Miltenyi-Biotec | 345110   | yes        |
| Mouse anti-human CD3               | 2    | Flow cytometry | APC-H7     | SK7         | 1:20         | BD Biosciences  | 560176   | yes        |
| Mouse anti-human CD4               | 2    | Flow cytometry | BUV395     | SK3         | 1:100        | BD Biosciences  | 563550   | yes        |
| Mouse anti-human CD8               | 2    | Flow cytometry | BUV496     | SK1         | 1:100        | BD Biosciences  | 741199   | yes        |
| Mouse anti-human TCR $\alpha\beta$ | 2    | Flow cytometry | BV750      | IP26        | 1:50         | BD Biosciences  | 747180   | yes        |
|                                    |      |                |            |             |              |                 |          |            |
| Rabbit anti-human CD4              | -    | IHC            | -          | SP35        | Ready-to-use | Roche Ventana   | 790-4423 | yes        |
| Rabbit anti-human CD8              | -    | IHC            | -          | SP57        | Ready-to-use | Roche Ventana   | 790-4460 | yes        |
| Mouse anti-human CD68              | -    | IHC            | -          | KP-1        | Ready-to-use | Roche Ventana   | 790-2931 | yes        |
| Mouse anti-human CD138             | -    | IHC            | -          | B-A38       | Ready-to-use | Roche Ventana   | 760-4248 | yes        |
| Rabbit anti-human CXCL7            | -    | IHC            | -          | poly-clonal | 1:20         | LSBio           | LS-B7394 | yes        |
| Rabbit anti-human CXCL12           | -    | IHC            | -          | poly-clonal | 1:40         | LSBio           | LS-B7489 | yes        |
| Mouse anti-human CXCR4             | -    | IHC            | -          | 12G5        | 1:50         | LSBio           | LS-B1986 | yes        |
| Rabbit anti-human Ki67             | -    | IHC            | -          | 30-9        | Ready-to-use | Roche Ventana   | 790-4286 | yes        |
| Mouse anti-human MUM1              | -    | IHC            | -          | MUM1P       | 1:50         | Agilent DAKO    | M7259    | Yes        |

\*Validated for the respective application according to the manufacturer's technical data sheet.

**Suppl. Table 7:** Number of cells in scRNA-seq before and after quality control

| PID | Sample       | # cells before filtering | # cells after filtering |
|-----|--------------|--------------------------|-------------------------|
| P01 | RBM_CD138pos | 4307                     | 2284                    |
| P01 | RBM_CD138neg | 2510                     | 1409                    |
| P01 | FL_CD138pos  | 3420                     | 2313                    |
| P01 | FL_CD138neg  | 3367                     | 2221                    |
| P02 | RBM_CD138pos | 6889                     | 4606                    |
| P02 | RBM_CD138neg | 3430                     | 2806                    |
| P02 | FL_CD138pos  | 8505                     | 6114                    |
| P02 | FL_CD138neg  | 5948                     | 3629                    |
| P03 | RBM_CD138pos | 6412                     | 3557                    |
| P03 | RBM_CD138neg | 6391                     | 3951                    |
| P03 | FL_CD138pos  | 2348                     | 1397                    |
| P03 | FL_CD138neg  | 7812                     | 5461                    |
| P04 | RBM_CD138pos | 4967                     | 4129                    |
| P04 | RBM_CD138neg | 7816                     | 5936                    |
| P04 | FL_CD138pos  | 2582                     | 2197                    |
| P04 | FL_CD138neg  | 5385                     | 3420                    |
| P05 | RBM_CD138pos | 3537                     | 1972                    |
| P05 | RBM_CD138neg | 6691                     | 5132                    |
| P05 | FL_CD138pos  | 2948                     | 1390                    |
| P05 | FL_CD138neg  | 5224                     | 3777                    |
| P06 | RBM_CD138neg | 4971                     | 3610                    |
| P06 | FL_CD138neg  | 4684                     | 3320                    |

RBM: random bone marrow; FL: focal lesion; CD138pos: CD138-enriched cells; CD138neg: CD138-depleted cells (negative fraction of CD138 sort)

**Suppl. Table 8:** Number of cells in scATAC-seq before and after quality control

| PID | Sample       | # cells before filtering | # cells after filtering |
|-----|--------------|--------------------------|-------------------------|
| P02 | RBM_CD138pos | 6110                     | 376                     |
| P02 | FL_CD138pos  | 985                      | 594                     |
| P03 | RBM_CD138pos | 914                      | 839                     |
| P03 | FL_CD138pos  | 201                      | 196                     |
| P04 | RBM_CD138pos | 1326                     | 1215                    |
| P04 | FL_CD138pos  | 623                      | 555                     |
| P05 | RBM_CD138pos | 3137                     | 2920                    |
| P05 | FL_CD138pos  | 2395                     | 2210                    |

RBM: random bone marrow; FL: focal lesion; CD138pos: CD138-enriched cells

**Suppl. Table 9:** Chromosomal regions used for supervised clustering of single-cell sequencing data

| PID | Sample | Regions with subclonal CNAs [in MBP]  |
|-----|--------|---|
| P01 | RBM    | 4 subclone solution by InferCNV was confirmed by WGS, no further clustering required                    |
| P01 | FL     | 4 subclone solution by InferCNV was confirmed by WGS, no further clustering required                    |
| P02 | RBM    | round1: chr6p (<25); round2: (chr6p+) chr19, (chr6p-) chr19   |
| P02 | FL     | round1: chr6p (<20); round2 (chr6p-): chr20; round3 (chr20-): chr19;<br>round4 (chr19+): chr4 (100-150) |
| P03 | RBM    | round1: chr11; round2: chr21; round3: chr4 (<105); round4: chr16 (>48)                                  |
| P03 | FL     | round1: chr11; round2: chr21; round3: chr4 (<105); round4: chr16 (>48)                                  |
| P04 | RBM    | round1: chr14+19q (cut into 6 clones); round2 Clone1-3 : chr13 (50-110), Clone4-6<br>chr13&chr14        |
| P04 | FL     | round1: chr14+19q (cut into 6clones); round2 Clone1,4 : chr13 (>45); Clone2,3,5,6<br>chr13+chr14        |
| P05 | RBM    | round1: chr8(<40); round2: chr7 (>100); round3: chr6 (<40)  |
| P05 | FL     | round1: chr8(<40); round2: chr7 (>100); round3: chr6 (<40)  |

RBM: random bone marrow; FL: focal lesion; CNA: copy number aberration; Mbp: Million base pairs; WGS: whole genome sequencing

Example for the supervised clustering approach (P05, presented in Fig. 2a):

- (1) P05 was first clustered based on chr8p (<40 Mbp)
  - Cells with del(8p): Subclone1
- (2) Cells without del(8p) were further clustered for chr7q (>100 Mbp)
  - Cells with gain(7q): Subclone2
- (3) Cells without gain(7q) were then clustered for chr6p (<40 Mbp)
  - Cells with gain(6p): Subclone3
  - Cells without gain(6p): Subclone4

## Supplementary References

- 1 Walker, B. A. *et al.* Identification of novel mutational drivers reveals oncogene dependencies in multiple myeloma. *Blood* **132**, 587-597, doi:10.1182/blood-2018-03-840132 (2018).
- 2 Yang, R. *et al.* Distinct epigenetic features of tumor-reactive CD8+ T cells in colorectal cancer patients revealed by genome-wide DNA methylation analysis. *Genome Biol* **21**, 2, doi:10.1186/s13059-019-1921-y (2019).